RESEARCH ARTICLE

Multilayer coating-assisted gold-encapsulated tilted fiber Bragg grating biosensor design

P. B. Prathap[1,2] · K. Saara[1]

Abstract To cope with up high rise in healthcare demands and accurate clinical decisions the fiber Bragg grating (FBG) sensors have performed superior over the traditional analog sensors for varied clinical decisions. The higher sensitivity and resolution toward accurate sensing make FBG a viable technology for clinical decision systems including biomechanical sensing, physiological sensing, non-invasive surgery, and biosensing. Depth assessment indicates that the encapsulated tilted FBG (TFBG), and surface plasmon resonance sensors have performed satisfactorily; yet, their suitability over the different operating conditions such as temperature, viscosity-change, noise, etc., remains suspicious. The at-hand biosensors fail to demodulate the response accurately once the surrounding refractive index approaches the cladding index. It requires a sufficiently large spectrum shift to demodulate and predict biosensing yield. To achieve it, in this paper, a multilayer coating-assisted gold-encapsulated TFBG biosensor is proposed. The proposed TFBG biosensor was designed with the grating angle of 10°, while gold encapsulation was done to improve resolution and sensitivity. To improve biosensing toward protein analysis and immunological assessment at first gold plating was done to improve reflectivity, while graphene oxide (GO) coating was done to enhance plasmonic attraction for biosensing. In function, GO coating served dual purposes including improved antibody and antigen absorption that helped sensitivity as well as yields sufficiently large spectra change to make detection decisions. More specifically, GO coating enables the trapping of the target molecules that eventually increases the refractive index of the coating material and hence undergoes a shift in the wavelength spectra, which is used for biosensing tasks. The higher refractive index of the coating material over the cladding index results in spectral shift and coupling wavelength shifts which helps target biosensing tasks. Simulations confirmed wavelength spectrum shift signifying biosensing tasks including protein analysis and immunological assessments for clinical decisions.

Keywords Fiber Bragg grating · Biosensor · Multilayer encapsulation · Surface plasmon resonance · Protein analysis · Immunological analysis

Introduction

The high pace rising global population and allied pressure on at-hand healthcare infrastructures including human experts have forced industry to achieve more automated and accurate diagnosis and medication solutions. Undeniably, healthcare innovations are going on across the horizon including pharmaceuticals, medicine, telemedicine, computer-aided diagnosis (CAD), etc. However, the development in hardware, especially sensor technologies has made diagnosis more time-efficient and scalable. The rising health complications have been demanding more accurate and reliable sensors to make early detection and diagnosis. This as a result can not only reduce mortality rate but can avoid further complications if diagnosed early and medicated on time. There are numerous complex healthcare practices such as cancer diagnosis, serum tests, protein analysis, etc., which demand reliable sensor solutions. Additionally, varied applications like biomechanical sensing, physiological

✉ K. Saara
    saara-ece@dsu.edu.in; saarakhamar@gmail.com

1   Department of Electronics and Communication Engineering, School of Engineering, Dayananda Sagar University, Bangalore 560114, India

2   Department of Electronics and Communication Engineering, Malnad College of Engineering, Hassan 573202, India

sensing, non-invasive surgery, and biosensing require highly sensitive sensors [1]. In the past, different analog sensors were developed and used for healthcare (sensing) purposes; however, the likelihood of compromised performance due to the local temperature change, interference, and strain can't be ruled out. Unlike traditional electrical sensors, optical sensors have performed superior due to high sensitivity, high resolution, and minimum impact of local conditions on sensing outputs [1]. Amongst the varied optical sensors, fiber Bragg grating (FBG) sensors have performed better across healthcare applications including biomechanical sensing, physiological sensing, non-invasive surgery, and biosensing. Undeniably, features like high sensitivity, chemical inertness, flexibility in use, and high scalability [1] make FBG a potential technology for aforesaid healthcare applications. Despite the aforementioned significance ensuring high resolution and sensitivity remains a challenge in biosensing, especially under the likelihood of local strain, interference, and temperature variation [1]. In this reference, over the last few years, different studies have been done on FBG designs where the authors have made efforts for better designs, materials, and structural optimization to improve sensitivity and resilience toward local impacts [2, 3].

In general, a biosensor can operate in both in vivo as well as ex vivo environments; however, the typical operating environments can be viscous, with liquids encompassing protein samples, blood samples, glucose, etc [1–3]. In this case, a biosensor requires to have higher sensitivity with low or negligible impact of the local ambiance [1–3]. On the contrary, the fact that the refractive index (η_{eff}) of the FBG biosensor can be affected because of the local temperature, stress, and viscosity conditions [4], and hence designing a suitable biosensor with high sensitivity and resolution becomes inevitable. To achieve it, the peak tracking method has performed well toward biosensing [5–8]; however, ensuring high resolution and sensitivity over diverse viscous and temperature conditions remains a challenge. Noticeably, FBG sensors are designed based on the periodic perturbation of certain designed effective RI (say, η_{eff}) by applying laser and interferometer setup [9]. In this mechanism, the structure of grating and corresponding Bragg shift is required to be designed optimally to retain the high accuracy and reliability of the peak-tracking-based biosensors. In reality, the majority of the classical interrogators show multiple and ambiguous peak spectra over the response signal and hence question the suitability of the FBG biosensor for clinical decisions [3, 9–11]. To alleviate such issues optimizing both grating structure as well as sensing-oriented materials is inevitable. For instance, in the past, the authors have performed grating encapsulation which improves surface immobilization toward the different bio-components (i.e., target protein, cells, antigens, etc.) [12, 13]. This as a result improves detection sensitivity and resolution [13]. A few

kinds of literature indicate that encapsulation with certain specific grating patterns and coating materials can achieve self-compensation ability along with higher sensitivity [3]. Additionally, it can alleviate issues like the impact of local temperature, strain, and viscosity [3].

Despite the efforts toward the different grating structures like long-periodic grating (LPG), phased grating FBG, super-structured FBG, and chirped FBG (CFBG) are found to be limited over the improved plasmonic FBG-biosensors [14]. This is mainly because of the larger refractive index sensitivity toward the thermal changes. As indicated above, the plasmonic biosensors are highly sensitive to the ROI changes because of the change in fluidic viscosity and strain that can influence peak-tracking accuracy [3, 15]. Recently, tilted FBG (TFBG) designs with grating-encapsulation [8, 16, 17] were proposed for biosensing [15, 18]. Yet, it requires a better ability to compensate for the ambiguous peaks and achieve high-resolution tracking. In a real-world scenario, TFBG is very sensitive to the change in the surrounding refractive index, especially when the aforesaid index value approaches the cladding index. In practical biosensing tasks, once the refractive index of the neighboring index approaches the cladding index, the attenuation bands shift toward shorter bandwidth particularly due to the sudden rise in the neighboring index. In this case, it becomes inevitable that the coupling wavelength must shift even though the surrounding (i.e., neighboring) index is more than the cladding index, which is highly probable over in vivo biosensing tasks. Considering a typical biosensing task of breast cancer detection or protein analysis, the attenuation bands might shift to the shorter wavelength because the neighboring index gets increased from the ambient value 1 (i.e., air index) to the larger value which is near the cladding index. It infers that the FBG turns out to be very sensitive to the change in the neighboring index, especially when the refractive index approaches the cladding index. It can also result shift in the coupling wavelength when the neighboring index is higher than the cladding index. To improve efficacy the grating can be coated with a suitable material that can be exposed to the external analyte that consequently can change the refractive index and hence can undergo a shift in transmission spectra. This approach can be applied to perform biosensing tasks.

Considering above above-stated inferences and allied scopes in this paper a novel and robust gold-encapsulated tilted fiber Bragg grating model is proposed. To improve sensitivity the proposed TFBG design was proposed with a grating angle of 10°, while gold encapsulation was done to improve the resolution and sensitivity of the proposed biosensor design. In the proposed biosensor design, the TFBG was processed for multilayer coating where at first gold plating was done to improve reflectivity. In contrast, graphene oxide (GO) coating was done on the inner core

to improve plasmonic attraction for better sensitivity and sensing resolution. Here, the key purpose of GO coating was to improve antibody and antigen absorption to enhance sensing resolution and sensitivity. In the proposed biosensor design, the refractive index of the coating material is higher than the cladding and hence once the effective refractive index approaches the neighboring index undergoes spectra change and coupling wavelength shifts, signifying the detection of the target molecule or antigen. Here, the selection of GO coating enables the trapping of the target molecules that eventually increases the refractive index of the coating material and hence undergoes a shift in the wavelength spectra, which is used to perform biosensing tasks. The simulation results and allied inferences indicate that the proposed biosensor shows higher resolution in terms of the high refraction index unit change, signifying its suitability for varied biosensing tasks including protein analysis and immunological assessment.

The other sections of this paper are given as follows. Sect. "Related work" discusses the related work, which is followed by the proposed model in Sect. "Research questions". Sect. "Proposed system" presents the proposed model, while the simulation results and allied research conclusions are discussed in Sect. "Results and discussion" and Sect. "Conclusion," respectively.

Related work

This section discusses some of the key kinds of literature about FBG biosensor designs.

In [19], Chen et al. proposed a plasmonic TFBG sensor with a grating angle of 18°. Additionally, they coated FBG with a 50 nm gold coating to improve biomolecule interaction detection in adenosyl-L-homocysteine. To improve sensitivity, they designed FBG with a spectrally dense comb having backward-propagating cladding resonance modes of Q-factor 10^{-4}. Eventually, they measured the spectral overlap between the excited cladding modes and absorption features to measure wavelength shifts. Sun et al. [20] proposed a reflective micro-FBG biosensor to detect free DNA hybridization. The authors designed the proposed biosensor with the layered self-structuring ability to quantify wavelength shifts between two well-defined resonances of micro-FBG. The use of poly-ethylenimine (PEI), poly-acrylic acid (PAA), and single-stranded DNA (ssDNA) as polyelectrolyte multilayer film helped to enhance temperature resilience. To further improve sensitivity, Korganbayev et al. [21] designed a TFBG sensor for ex vivo laser ablation purposes. TFBG sensor underwent neighboring RI change for sucrose concentrations and thus showed different peaks over response spectra. Gold encapsulation was proposed by

Lobry et al. [8] to design plasmonic FBG for peak-tracking-based biosensing. The authors designed a demodulator that exploited the intersection of the upper and lower envelopes of the gold-coated TFBG spectra to improve HER2 (Human Epidermal Growth Factor Receptor-2) protein detection for breast cancer diagnosis. In [12], graphene oxide (GO) was applied as a coating material for TFBG biosensor design for staphylococcal protein assessment for human immunoglobulin G (IgG) analysis. Duan et al. [22] proposed a plasmonic TFBG sensor by applying thymine (T)-Hg -thymine (T) (T-Hg-T) base asymmetric pairing and Au nanoparticles (AuNPs) to detect ultra-low Hg 2 + concentration. In [23], the TFBG biosensor was designed with GO coating for bovine serum albumin (BSA) immune-sensing. González-Vila et al. [13] proposed an optical power-based interrogator for plasmonic TFBG biosensor. An FBG-based catheter was designed by Beisenova et al. [24] for epidural anesthesia. Unlike TFBG, a chemically etched biosensor was designed by Bekmurzayeva et al. [25], while a linearly-CFBG microwave photonic model was proposed in [26] for biosensing tasks. Yet, such solutions might suffer resonance behavior and inappropriate RIU sensitiveness [27]. In [28], used multifunctional three-dimensional nano-flower to design TFBG biosensor. They designed it with TFBG with zinc oxide (ZnO) nanoflower. Even though the authors applied a silane coupling-based self-structuring model along with polyelectrolyte ZnO coating on TFBG, they failed to address local interference and temperature and its impact on sensitivity. Gao et al. [29] on the other hand proposed a Co2 + -doped TFBG biosensor for carcinogen detection. Noticeably, they considered a tilt angle of 8° where grating was inscribed into Co2 + doped fiber. Wang et al. [30] designed a sandwich (plasmonic) TFBG biosensor by using *p*-mercaptophenylboronic acid (PMBA) monolayer and Au nanoparticles (AuNPs). In this design, the TFBG sensor was immobilized in conjunction with a PMBA monolayer that improved sensitivity toward glucose detection. Leitão et al. [17] designed gold-encapsulated TFBG for plasmonic immunosensor. Liang et al. also designed [31] TFBG SPR biosensors for protein assessment. More specifically, the authors used cysteamine hydrochloride to trap rabbit IgG antigen molecules on the surface of gold encapsulation for goat anti-rabbit IgG antibody detection.

Research questions

In sync with the overall research goals and allied scopes, this research defines certain questions. These research questions are:

RQ1 Can the use of the TFBG structure be effective toward accurate biosensing tasks under different operating conditions?

RQ2 Can the use of TFBG structure with multilayer coating be effective toward biosensing tasks?

RQ3 Can the strategic amalgamation of gold encapsulation and graphene oxide coating enable higher reflectivity (and sensitivity) and plasmonic absorption toward highly sensitive and accurate biosensing tasks?

Thus, the overall research intends to achieve answers to these key research questions that eventually can put the foundation for a robust biosensor design.

Proposed system

This section primarily discusses the overall proposed model and allied implementation toward designing a reliable and sensitive biosensor design.

Unlike traditional biosensor designs, where we have applied traditional FBG structure with certain encapsulations to improve plasmonic absorption for biosensing tasks, the proposed biosensor focuses on optimizing both grating structures as well as a coating to ensure superior sensitivity and accuracy. Recalling the fact that the use of TFBG structure can yield high resolution and sensitivity toward biosensing, we applied it as a base structure to design and improve the proposed biosensor solution [32]. For a robust biosensor design improving sensitivity and resolution as well as the target (say, biosensing tasks) specific peak tracking or spectral change can be of paramount significance. With this motivation, in this work, a multilayer coating approach was considered where each layer and allied material was selected to perform or catalyze a specific task. More specifically, the proposed FBG biosensor was designed as a tilted grating structure that induces reflection for better peak tracking or spectral analysis. We designed TFBG with tilt-grating where we considered the grating angle of 10° that improves peak tracking performance. To further improve efficacy, we modeled upper cladding encapsulation by using gold (Au) coating material.

In the proposed design, gold coating or gold encapsulation was done for the grating length of 10 mm. Being a multilayer coating structure to retain high reflectivity at first gold encapsulation was done, where we maintained the layer width at 0.01 mm. Moreover, it was done to improve biomolecule interaction detection that consequently can increase surface density and viscosity. It consequently can increase the refractive index in cladding mode and hence can result in quantifiable wavelength shifts for biosensing tasks. Subsequently, to improve plasmonic absorption and target molecule attraction in this work a thin layer of graphene oxide (GO) is deposited

in cladding over the grating length. Here, we selected GO coating that attracts the molecules about the proteins and varied immunological artifacts. The proposed coating serves dual tasks encompassing antibody and antigen absorption which can enable improved sensitivity and hence can yield sufficiently large spectral changes for accurate detection. In the proposed TFBG design, GO coating enables trapping of the target molecules that eventually increase neighboring refractive index and hence undergo wavelength shift toward cladding. This change in spectral behavior and allied peak tracking enables targeted biosensing tasks including protein analysis (ex. Staphylococcal) and immunological analysis. A snippet of the overall proposed multilayer coating-assisted TFBG biosensor is given in Fig. 1.

An illustration (schematic) of the proposed TFBG biosensor is depicted in Fig. 1. As depicted in Fig. 1, the tilt grating is modeled at an angle of 10°, while the grating length was maintained at 10 mm. Since, in this work MATLAB simulation is done and fabrication is beyond the current scope the design parameters along with functional details are given in this section. However, for real-time realization and fabrication, the aforementioned design can be fabricated with the hydrogen-loaded single-mode fiber such as the corning fiber model SMF-28. However, the simulation model is designed with a core diameter of 8.2 μm, while the cladding diameter was maintained at 125 μm. To fabricate the same design scanning phase-mask technique can be taken into consideration. Noticeably, the phase masking technique represents a laser beam passing across a phase or amplitude mask, which is applied as a diffractive optical element that divides the incoming beam into two diffraction orders (say, +1 and −1) having equal power levels.

As stated earlier, to improve reflectivity 0.01 mm gold coating is modeled on the cladding surface (which can be done by performing the ion-beam sputtering technique). In this manner, functionally a fraction of the transmitted light passes through the grating, which is subsequently coupled into the cladding to yield a large quantity of cladding modes. Now, in conjunction with the phase-matching criteria, for the
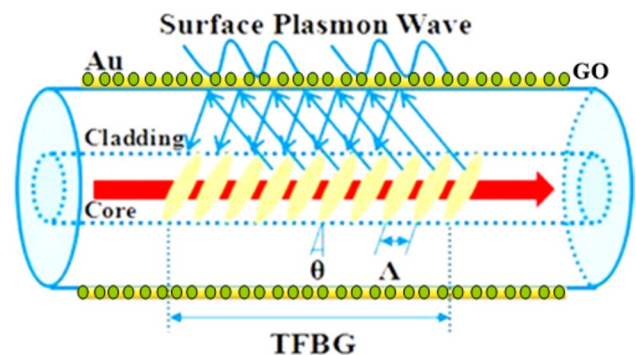

Fig. 1 Proposed multilayer coating assisted TFBG biosensor design

proposed biosensor we derive the resonant wavelength for the $i-th$ cladding mode by applying (1).

$$\lambda^i_{\text{coupling}} = \left(\eta_{\text{eff·CORE}} + \eta^i_{\text{eff–CLAD}}\right)\Lambda / \cos\theta \tag{1}$$

In (1), $\eta_{\text{eff·CORE}}$ is the effective refractive index of the core mode, while the effective refractive index for the $i-th$ cladding mode is given by $\eta^i_{\text{eff–CLAD}}$. The other parameters Λ and θ are the grating period and the tilt angle, correspondingly. Now, in conjunction with the design construct and condition that the surface plasmon wave on the upper surface film is excited, the cladding model satisfying the phase-matching criteria and dispersion are coupled (with the aforesaid surface plasmon wave). In this case, there would be the emergence of surface plasmon resonance, especially on the interface of the gold layer or interface or medium. Subsequently, the energy of the cladding mode gets transferred to the surface plasmon waves which consequently decreases the energy of the associated cladding mode in the transmission spectrum. It eventually results in a concave region [33]. It indicates that the surface plasmon waves often remain sensitive to the neighboring refractive index and its changes. With the change in the effective refractive index, there used to be a spectral shift, and hence the wavelength and magnitude of the surface plasmon resonance changes. It eventually changes the value of $\lambda^i_{\text{coupling}}$. In this reference, the surrounding refractive index can be estimated by detecting the change in peaks of the surface plasmon wavelength and its magnitude [34, 35].

As depicted in Fig. 1, in the proposed biosensor design, in addition to the gold encapsulation graphene oxide coating was also done to improve target molecule or plasmonic absorption. In this manner, the functional group present in GO gets ionized in the test solution (say, protein or other immunological assessment samples) which eventually yields the negative ion of the surface of GO. In this manner, it traps the molecules by immobilizing them due to the covalent and non-covalent bonds, and electrostatic interactions. In other words, the use of GO coating acts as a plasmonic absorption layer and thus immobilizes target molecules and thus undergoes increased density. This increase in density eventually impacts the refractive index and therefore induces wavelength shift and hence makes peak-tracking more sensitive toward biosensing [36].

For a real-time biosensing task, as the molecular orientation of the antibodies remains at random (at the surface), it becomes feasible to immobilize the antibody structure on the sensor surface (due to antigen binding capability). It eventually decreases the antigen–antibody binding efficacy. The target protein molecule or varied other immunological assessment molecules possess higher affinity toward the antibody molecule's Fc regions. These protein molecules get manipulated on the sensor surface, which is then followed by directional immobilization of the antibodies on the sensor surface. As a result, the binding sites of the Fab region about the antibody molecules get elongated outward [37] eventually enhancing the binding efficacy of the antigen–antibody and thus improving sensing sensitivity. The protein molecules and GO can immobilize a larger fraction of antibodies directionally on the metal surface which consequently can improve sensing sensitivity. Noticeably, the fabrication mechanism of the biosensor is the same as that of the GO-coated TFBG surface plasmon resonance biosensor. However, the decisive disparity is that the protein or test solution is required to be injected into a glass tube to soak the sensing area at normal room temperature for 30 min. However, it can be done post-activation of the carboxyl groups of GO, which can later be injected into the rabbit antihuman IgG solution to ensure better antibody immobilization.

In our case, due to the plasmonic absorption $\eta_3 > \eta_{\text{CLAD}}$, the cladding mode doesn't undergo any internal reflection and hence behaves as a leaky mode FBG. The fiber then acts as a circular dielectric waveguide. Let, a_2 be the radius of the cladding mode, and η_d be the index about the cladding index, and η_3 or η_s be the surrounding index or coating material (post absorption) index. Then, in this case, the parameters $\beta_{\text{CLAD}}, u_2, w_2,$ and v possess complex values and hence the Bessel functions might have complex arguments. On the other hand, if the propagation constant β_{CLAD} turns out to be complex, then it becomes significant to consider leaky modes. Now, in a single-mode fiber, the proposed TFBG can couple the fundamental core mode to the co-propagating cladding mode at the coupling wavelength given by (2).

$$\lambda^{(n)}_i = \left(\eta_{\text{core}}(\lambda_i) - \eta^{(n)}_{\text{CLAD}}(\lambda_i)\right)\Lambda \tag{2}$$

In (2), $\lambda^{(n)}_i$ is the nth coupling wavelength, while $\eta_{\text{core}}(\lambda_i)$ indicates the effective refractive index of the core. $\eta^{(n)}_{\text{CLAD}}(\lambda_i)$ Is the effective refractive index of the nth cladding model, while Λ states the grating period. It indicates that whenever η_3 changes due to the absorption of the target molecule in GO coating, the propagation constant of cladding modes $\beta^{(n)}_{\text{CLAD}}$ and the refractive index of cladding model $\eta^{(n)}_{\text{CLAD}}(\lambda_i)$ changes that consequently would cause coupling wavelength $\lambda^{(n)}_i$ shift. We measured this wavelength shift to assess the biosensing task.

Demodulating spectral shift

As stated above due to the absorption of the target molecule the surrounding refractive index (say, η_s) characterizing the refractive index of the outer surface area changes that consequently results in the coupling wavelength shift. In

addition to the said wavelength shift it also causes changes in the transmission amplitude. In our proposed work, we derived a mathematical model to quantify the change in amplitude as well as spectral shift for accurate biosensing. More specifically, we calculated the three-layer cladding modes that comprise core, cladding, and surrounding indices. Inheriting Erdogan's formulation [38], the three-layer cladding modes can be derived as (2).

$$\xi_0 = \xi_0' \tag{3}$$

where,

$$\xi_0 = \frac{1}{\sigma^2} \frac{u_2\left(\frac{(JK+\sigma_1 u_{21} u_{23})}{\eta_2^2 a_1 a_2}\right)p_l(a_2) - Kq_l(a_2) + Jr_l(a_2) - \frac{1}{u_2}s_l(a_2)}{-u_2\left(\frac{u_{32}}{\eta_2^2 a_2}J - \frac{u_{21}}{\eta_1^2 a_1}K\right)p_l(a_2) + \frac{u_{32}}{\eta_2^2 a_2}q_l(a_2) + \frac{u_{21}}{\eta_1^2 a_1}r_l(a_2)}. \tag{4}$$

$$\xi_0' = \sigma_1 \frac{u_2\left(\frac{u_{32}}{a_2}J - \frac{\eta_3^2 u_{21}}{\eta_2^2 a_1}K\right)p_l(a_2) - \frac{u_{32}}{a_2}q_l(a_2) - \frac{u_{21}}{a_1}r_l(a_2)}{u_2\left(\frac{\eta_3^2}{\eta_2^2}JK + \frac{\sigma_1 \sigma_2 u_{21} u_{32}}{\eta_2^2 a_1 a_2}K\right)p_l(a_2) - \frac{\eta_3^2}{\eta_1^2}Kq_l(a_2) + Jr_l(a_2) - \frac{\eta_2^2}{\eta_1^2 u_2}s_l(a_2)}. \tag{5}$$

The definitions of the key variables are given as follows:

$$\sigma_1 = il^{n_{eff}}/Z_0 \tag{6}$$

$$\sigma_2 = il\eta_{\text{eff}Z_0} \tag{7}$$

$$Z_0 = \sqrt{\mu_0/\varepsilon_0} = 337\ \Omega \tag{8}$$

$$u_{21} = \frac{1}{u_2^2} - \frac{1}{u_1^2} \tag{9}$$

$$u_{32} = \frac{1}{w_3^2} + \frac{1}{u_2^2} \tag{10}$$

$$u_1^2 = (2\pi/\lambda)^2\left(\eta_1^2 - \eta_{\text{eff}}^2\right) \tag{11}$$

$$u_2^2 = (2\pi/\lambda)^2\left(\eta_2^2 - \eta_{\text{eff}}^2\right) \tag{12}$$

$$w_3^2 = (2\pi/\lambda)^2\left(\eta_{\text{eff}}^2 - \eta_3^2\right) \tag{13}$$

$$J = \frac{J_l'(u_1 a_1)}{u_1 J_l(u_1 a_1)} \tag{14}$$

$$K = \frac{K_l'(w_3 a_2)}{w_3 K_l(w_3 a_2)} \tag{15}$$

$$p_l(r) = J_l(u_2 r)N_l(u_2 a_1) - J_l(u_2 a_1)N_l(u_2 r) \tag{16}$$

$$q_l(r) = J_l(u_2 r)N_l'(u_2 a_1) - J_l'(u_2 a_1)N_l(u_2 r) \tag{17}$$

$$r_l(r) = J_l'(u_2 r)N_l'(u_2 a_1) - J_l(u_2 a_1)N_l'(u_2 r) \tag{18}$$

$$s_l(r) = J_l'(u_2 r)N_l'(u_2 a_1) - J_l'(u_2 a_1)N_l'(u_2 r) \tag{19}$$

In the above equations, the parameter l signifies the azimuthal number, while J_l, N_l be the $l - th$ order Bessel functions of the first and the second types, correspondingly.

The other parameters like I_l and K_l are the $l - th$ order modified Bessel functions of the 1st and the 2nd types, correspondingly.

The recursive functions controlling the aforesaid Bessel and the modified Bessel functions [39] are given as follows:

$$J_{l+1}(u_i r) = -J_l'(u_i r) + (l/u_i r)J_l(u_i r) \tag{20}$$

$$J_{l-1}(u_i r) = J_l'(u_i r) + (l/u_i r)J_l(u_i r) \tag{21}$$

$$N_{l+1}(u_i r) = -N_l'(u_i r) + (l/u_i r)N_l(u_i r) \tag{22}$$

$$N_{l-1}(u_i r) = N_l'(u_i r) + (l/u_i r)N_l(u_i r) \tag{23}$$

$$K_{l+1}(w_i r) = -K_l'(w_i r) + (l/w_i r)K_l(w_i r) \tag{24}$$

$$K_{l-1}(w_i r) = -K_l'(w_i r) - (l/w_i r)K_l(w_i r) \tag{25}$$

Thus, applying the above-discussed core and cladding mode functions, we derived a MATLAB model that measured and plotted the wavelength shift when the surrounding refractive index increases. In other words, we quantify the change in wavelength shift and peaks (due to the change in amplitude) once the refractive index of the cladding more approaches the neighboring index or the surrounding refractive index η_s (here, or $\eta_3 = \eta_s$).

Results and discussion

In this paper, a multilayer coating-assisted TFBG biosensor was proposed. More specifically, the proposed biosensor was designed in such a manner that it achieves higher sensitivity and accuracy to make the solution reliable and scalable toward clinical decisions. The proposed design embodied tilted Bragg grating with a grating length of 10 mm. The grating angle was maintained at 10°. Subsequently, the cladding encapsulation was done with a gold layer of 0.01 mm. Here, the gold-encapsulation was done to improve reflectivity and hence accurate peak tracking for the amplitude and wavelength shift analysis. Furthermore, to enable biosensing ability, especially protein analysis and other (similar) immunological assessments Graphene Oxide (GO) coating was done. Here, GO acted as a plasmonic absorption layer. In this manner, the layered amalgamation of gold and GO was applied to achieve higher reflectivity, sensitivity, and high-resolution detection. Recalling the fact that, unlike traditional FBG structures, the use of tilted FBG can help achieve superior sensitivity and reflectivity to gain high-resolution yields. For simulation, MATLAB scripts were modeled, where the core refractive index was maintained at 1.4 (η_1), while the cladding refractive index was fixed at 1.45 (η_2). The proposed multilayer encapsulation by using gold and GO coating was quantified to have increased the refractive index and hence it was fixed at 1.458 (η_3). To be noted, the proposed GO coating caused trapping of the target protein molecules that increases surrounding refractive index (η_3) and therefore is hypothesized to undergo wavelength shift as well as change in spectral amplitude change that puts the foundation for biosensing. Since, in this research, no physical fabrication or experimental assessment was done, we simulated our proposed design with the different refractive indices emulating the real-time plasmonic absorption phenomenon and resulting change in the surface or surrounding refractive index. The proposed TFBG biosensor was designed by using MATLAB software. The simulation was done on a central processing unit armored with Microsoft Operating System functional with Intel-i5 processor, 3.2 GHz processor, and 8 GB memory. Noticeably, the overall performance characterization is done by simulating the proposed structure and hence fabrication and allied laboratory (experimental) analysis is beyond the scope of this work.

As hypothesized to assess the robustness of the proposed biosensor, performance characterization is done in terms of the wavelength shift over changing surrounding refractive index (say, the refractive index at the surface of coating material). Elaborating the aforesaid hypothesis that increasing target molecular absorption at the interface or coating surface would increase density and hence the refractive
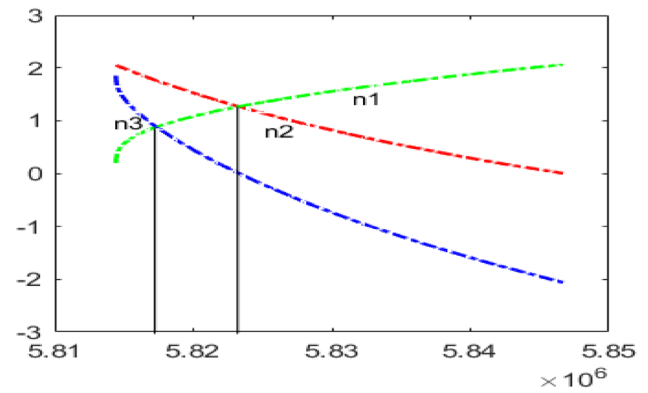

Fig. 2 The zero-crossings analysis for the solution HE_{11} mode

index (i.e., η_3). This eventually would result in coupling wavelength shift as well as reduced amplitude. In this reference, we have examined the efficacy of the proposed biosensor design in terms of the wavelength shift, transmission (dB) power versus wavelength (λ), and zero-crossing point shift. A detailed discussion of the results obtained is given as follows:

Before discussing the spectral shift toward biosensing characterization, the crossover points over the different modes are depicted in Fig. 2. In this work, we considered graphical analysis to characterize crossover points for the different modes. This approach depicts the curse against the real axis to generate feasible zero-crossings. Let, the Eq. (26)

$$u\frac{J_1(u)}{J_0(u)} = w\frac{K_1(w)}{K_0(w)} \tag{26}$$

where, the variables $u^2 = k\eta_1^2 - \beta^2$ and $w^2 = \beta^2 - k\eta_2^2$. In conjunction with the aforesaid left-hand and right-hand side values for the different modes, the graphical outputs are obtained (Fig. 2). In this analysis, we considered $\eta_1 = 1.4$, $\eta_2 = 1.45$ and $\eta_3 = 1.458$, pre-conditioned at $\eta_2 k < \beta < \eta_1 k$.

Observing the result (Fig. 2), it can be found that for η_1 and η_2 the crossing point exists at the 5.823×10^6, where the value of the core and cladding mode refractive indices are 1.4 and 1.45, correspondingly. On the contrary, at the cladding mode refractive index approaches the surrounding or surface refractive index (i.e., the surface of the coating material) $\eta_3 = 1.458$, and the crossing point converges earlier, which is 5.817×10^6. Here, the points where these curves (i.e., η_1 and η_2) cross pertaining to the HE_{11} core mode, while η_2 and η_3 depict the cladding mode. It depicts that the moment the cladding index approaches the surrounding refractive index η_3 it undergoes earlier zero-crossing, which can be considered for biosensing decision. In conjunction with the aforesaid inferences, we assumed that the target molecular absorption at the coating surface over a
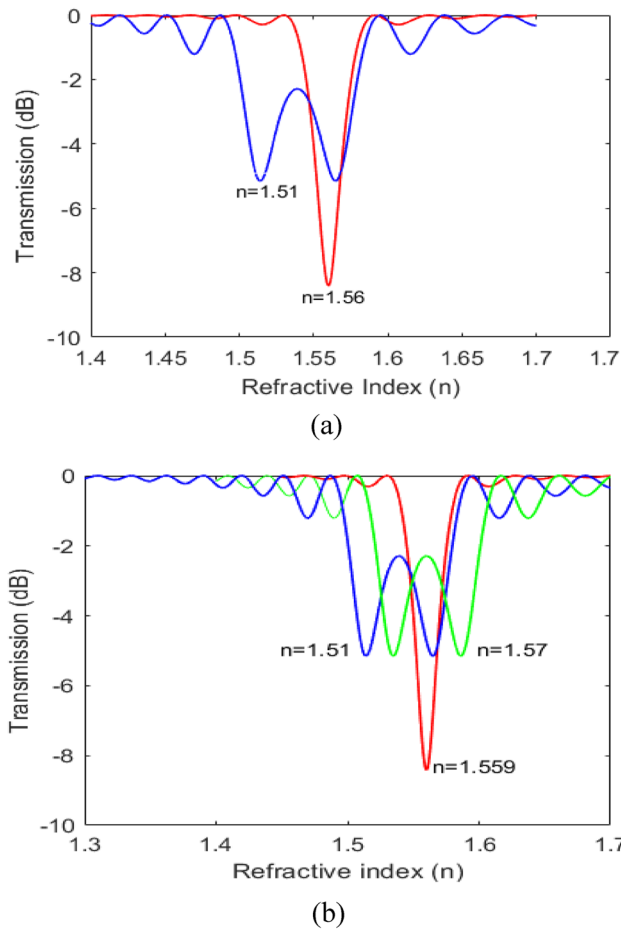
(a)

(b)

Fig. 3 **a**, **b** Transmission spectrum for the different refractive indices

Fig. 4 Coupling wavelength shift over the change in surrounding refractive indices

longer period such as one house can increase the surrounding refractive index (i.e., η_3 or η_s). Therefore, we simulated the spectral outputs for the different surrounding indices (η_3 =1.51 and 1.56). The results obtained are given in Fig. 3.

The result (Fig. 3) indicates that increasing surface or surrounding refractive index of the TFBG sensor results quantifiably sufficient wavelength shift and amplitude change. In sync with the hypothesis that the plasmonic absorption at the coating surface results increase in density and hence the refractive index. Interestingly, the result (Fig. 3b) indicates a contrast output signifying that the exceedingly high refractive index saturates transmission spectra (dB). In other words, the spectral output at $\eta = 1.51$ turns out to be the same as that of $\eta = 1.57$. Noticeably, with exceedingly high saturation or density (it can be due to the excessive molecular absorption at the cladding mode or the coating surface), there can be zero internal reflection thus making fiber core as normal dielectric hollow cylinder that results similar spectra as that of $\eta = 1.51$. It clearly indicates that the selection of the coating material must be done in such manner that it provides ambiguity-free spectral outputs. In
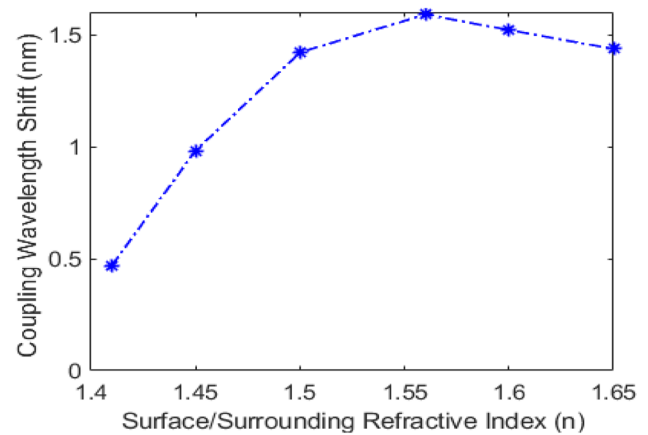
this reference, we considered gold encapsulation as a metal layer followed by GO coating for plasmonic absorption. In real-world testing, the protein sample can be injected into the surface which can be soaked for some period (in minutes, based on the solution intake). Here, the solution type and its composition can be selected based on certain calibration and clinical standards [8, 12]. The result indicates that the use of GO coating as a molecular absorbent can increase the surrounding refractive index from 0.5 to 1. Therefore, the soaking period or injection volume can be decided accordingly such that the effective refractive index change and allied amplitude (and coupling wavelength spectral change) can be visualized clearly. In summary, with the suitable concentration and coating area the proposed design can yield sufficiently large spectral shift and allied amplitude (in dB) changes, which can be considered for biosensing tasks. This inference is re-confirmed by assessing the change or shift in the coupling wavelength (λ). The following result (Fig. 4) indicates that with the change in the surrounding refractive index (say, the surface surrounding index) the quantifiable shift in the coupling wavelength (λ) takes place, which can be quantified for biosensing purposes.

In this manner, the overall results obtained confirm that the use of our proposed multilayer coating-assisted TFBG biosensor can be used for varied biosensing tasks including protein analysis and other immunological assessments. The overall research conclusion and allied inferences are given in the subsequent section.

Conclusion

In this paper, a novel and robust multilayer coating-assisted TFBG biosensor was proposed. Unlike traditional FBG solutions, this research work focused on improving

sensitivity and resolution by improving grating structures as well as coating and encapsulation. The proposed TFBG was designed with a grating angle of 10° that enabled higher sensitivity and resolution to serve biosensing tasks. Unlike standalone grating encapsulation such as gold coating, the proposed biosensor encompassed multilayer coating encompassing gold and graphene oxide (GO) coatings. Here, at first gold encapsulation was done with the 0.01 mm layer width to enhance reflectivity and hence sensitivity. Subsequently, GO coating was modeled to improve antibody and antigen absorption or plasmonic attraction which helped not only to improve sensitivity but increased refractive index and hence yielded sufficiently large spectral changes to perform biosensing. Here, the amalgamation of Gold and GO improved both sensitivities as well as resilience to local conditions such as temperature. The simulation and allied performance characterization revealed that the proposed biosensor shows a sufficiently large wavelength shift toward the neighboring index revealing the presence of the target molecule. The higher refractive index per unit change signifies the efficacy of the proposed biosensor toward varied biosensing tasks including protein analysis and immunological assessment. Though, in this paper GO coating was done to improve plasmonic absorption to serve protein analysis and immunological assessment. However, in the future other coating material(s) can be applied toward cancer detection. To improve temperature and noise resilience films like polyethylenimine (PEI) and polyacrylic acid (PAA) can be applied to serve scalable biosensing tasks.

Declarations

References

1. A.G. Leal-Junior, C.A.R. Diaz, L.M. Avellar, M.J. Pontes, C. Marques, A. Frizera, Polymer optical Fiber sensors in healthcare applications: A comprehensive review. Sensors **19**(14), 3156 (2019)
2. W. He, D. Goodkind, P. Kowal, *International Population Reports: an Aging World: 2015* (US Census Bureau, Suitland-Silver Hill, MD, USA, 2016), p.95
3. D. Lo Presti et al., Fiber Bragg gratings for medical applications and future challenges: a review. IEEE Access **8**, 156863–156888 (2020)
4. D. Sharma, G.S. Aujla, R. Bajaj, Evolution from ancient medication to human-centered healthcare 4.0: a review on health care recommender systems. Int. J. Commun. Syst. **36**, 4058 (2019)
5. W. Xu, D. Wang, D. Li, C.C. Liu, Recent developments of electrochemical and optical biosensors for antibody detection. Int. J. Mol. Sci. **21**(1), 134 (2019)
6. C. Chen, J. Wang, Optical biosensors: an exhaustive and comprehensive review. Analyst **145**(5), 1605–1628 (2020)
7. X.D. Wang, O.S. Wolfbeis, Fiber-optic chemical sensors and biosensors (2015–2019). Anal. Chem. **92**(1), 397–430 (2020)
8. M. Lobry et al., Plasmonic fiber grating biosensors demodulated through spectral envelopes intersection. J. Lightwave Technol. **39**(22), 7288–7295 (2021)
9. C. Massaroni, P. Saccomandi, D. Formica, D. Lo Presti, M.A. Caponero, G. Di Tomaso, F. Giurazza, M. Muto, E. Schena, Design and feasibility assessment of a magnetic resonance-compatible smart textile based on fiber Bragg grating sensors for respiratory monitoring. IEEE Sens. J. **16**(22), 8103–8110 (2016)
10. R. Correia, S. James, S.W. Lee, S.P. Morgan, S. Korposh, Biomedical application of optical fiber sensors. J. Opt. **20**(7), 73003 (2018)
11. M.D. Al-Amri, M. El-Gomati, M.S. Zubairy, *Optics in Our Time* (Springer, Cham, Switzerland, 2016)
12. Q. Wang, J.-Y. Jing, B.-T. Wang, Highly sensitive spr biosensor based on graphene oxide and staphylococcal protein a comodified TFBG for human IgG detection. IEEE Trans. Instrum. Meas. **68**(9), 3350–3357 (2019)
13. Á. González-Vila, A. Lopez-Aldaba, D. Kinet, P. Mégret, M. Lopez-Amo, and C. Caucheteur, Optical power-based interrogation of plasmonic tilted fiber Bragg grating biosensors, in 25th Optical Fiber Sensors Conference (OFS), (2017), pp. 1–4,
14. L. Han et al., Specific Detection of Aquaporin-2 Using Plasmonic Tilted Fiber Grating Sensors. J. Lightwave Technol. **35**(16), 3360–3365 (2017)
15. T. Guo, F. Liu, B.-O. Guan, J. Albert, Tilted Fiber grating mechanical and biochemical sensors. Opt. Laser Technol. **78**, 19–33 (2016)
16. C. Massaroni, M. Zaltieri, D. Lo Presti, A. Nicolò, D. Tosi, E. Schena, Fiber Bragg grating sensors for cardiorespiratory monitoring: a review. IEEE Sens. J. **21**(13), 14069–14080 (2021)
17. C. Leitão et al., Cortisol in-fiber ultrasensitive plasmonic immuno-sensing. IEEE Sens. J. **21**(3), 3028–3034 (2021)
18. T. Guo, Á. González-Vila, M. Loyez, C. Caucheteur, Plasmonic optical fiber-grating immune-sensing: a review. Sensors **17**(12), 2732 (2017)
19. X. Chen et al., In-situ detection of small biomolecule interactions using a plasmonic tilted fiber grating sensor. J. Lightwave Technol. **37**(11), 2792–2799 (2019)
20. D. Sun, T. Guo, B.-O. Guan, Label-free detection of DNA hybridization using a reflective microfiber Bragg grating biosensor with self-assembly technique. J. Lightwave Technol. **35**(16), 3354–3359 (2017)
21. S. Korganbayev, M. De Landro, A. Wolf, D. Tosi, P. Saccomandi, Tilted fiber Bragg grating measurements during laser ablation of hepatic tissues: quasi-distributed temperature reconstruction and cladding mode resonances analysis. IEEE Sens. J. **22**(16), 15999–16007 (2022)
22. Y. Duan et al., TFBG-SPR DNA-biosensor for renewable ultratrace detection of mercury ions. J. Lightwave Technol. **39**(12), 3903–3910 (2021)
23. Y. Wang et al., Immunosensor Based on Cladding-etched Excessively Tilted Fiber Grating Coated with Graphene Oxide, in 2019 18th International Conf. on Optical Communications and Networks (ICOCN), (2019), pp. 1–3
24. A. Beisenova, A. Issatayeva, C. Molardi, and D. Tosi, Fiber Bragg Grating Sensor-Based Optical Guidance System for Epidural Catheter, in 2018 IEEE Sensors, (2018), pp. 1–4
25. A. Bekmurzayeva, M. Shaimerdenova and D. Tosi, "Fabrication and Interrogation of Refractive Index Biosensors Based on Etched Fiber Bragg Grating (EFBG)," 2018 40th Annual

International Conference of the IEEE Engg. In Medicine and Biology Society (EMBC), pp. 4289–4292, (2018)

26. O. A. Stepustchenko, R. A. Eshpay, I. U. Kurbiev, A. D. Proskuriakov, and V. V. Kadushkin, LC-FBG-Based Microwave Photonic System for Refractometric Biosensors, in 2020 Systems of Signal Synchronization, Generating and Proc. in Telecomm. (SYNCHROINFO), (2020), pp. 1–6

27. O. G. Morozov, I. I. Nureev, A. Z. Sahabutdinov, R. R. Gubaidullin, and G. A. Morozov, "Problem of Fano Resonance Characterization in Ring pi-shift Fiber Bragg Grating Biosensors," 2019 Systems of Signal Synchronization, Generating and Proc. in Telecom., (2019), pp. 1–6

28. Y. Sun et al., Novel bio-sensing platform based on TFBG and multifunctional 3D nanoflower, in 2021 19th International Conference on Optical Communications and Networks (ICOCN), (2020), pp. 1–3

29. R. Gao, J. Ye, X. Xin, An integrated biological analysis and flow rate sensing for the real-time detection of carcinogen in water based on Co2+-doped optical fibers. IEEE Sens. J. **20**(4), 1912–1921 (2020)

30. F. Wang et al., PM level and large dynamic range glucose detection based on a sandwich type plasmonic fiber sensor. J. Lightwave Technol. **39**(12), 3882–3889 (2021)

31. P. Liang, Q. Jiang, and T. Zhang, Researches and experiments on reflective TFBG-SPR biosensor, in 2017 Chinese Automation Congress (CAC), (2017), pp. 1158–1162

32. P. B. Prathap, K. Saara, Self-compensating gold-encapsulated tilted fiber Bragg grating for peak tracking based biosensing applications. J. Opt. (2023). https://doi.org/10.1007/s12596-023-01369-6

33. J.-M. Renoirt, M. Debliquy, J. Albert, A. Ianoul, C. Caucheteur, Surface plasmon resonances in oriented silver nanowire coatings on optical fibers. J. Phys. Chem. C **118**(20), 11035–11042 (2014)

34. X. Qiu, X. Chen, F. Liu, B.-O. Guan, T. Guo, Plasmonic fiber-optic refractometers based on a high Q-factor amplitude interrogation. IEEE Sensors J. **16**(15), 5974–5978 (2016)

35. M.Z. Alam, J. Albert, Selective excitation of radially and azimuthally polarized optical fiber cladding modes. J. Lightw. Technol. **31**(19), 3167–3175 (2013)

36. J.N. Dash, R. Jha, Temperature insensitive PCF interferometer coated with graphene oxide tip sensor. IEEE Photon. Technol. Lett. **28**(9), 1006–1009 (2016)

37. J. Zhang, Y. Sun, Q. Wu, H. Zhang, Y. Bai, D. Song, A protein A modified Au-graphene oxide composite as an enhanced sensing platform for SPR-based immunoassay. Analyst **138**(23), 7175–7181 (2013)

38. T. Erdogan, Cladding Mode resonances in short-and long-period fiber grating filters. J. Opt. Soc. Am. **14**(8), 1760–1773 (1997)

39. C. Tsao, *Optical Fiber Waveguide Analysis* (Oxford University Press, Oxford, 1992)